Power Network Fault Location Based on Voltage Magnitude Measurements and Sparse Estimation

Yuxuan Zhu[1], *Student Member, IEEE,* Yixiong Jia[1], Yu Liu[1,2,*], *Senior Member, IEEE,* and Dayou Lu[1]
1. School of Information Science and Technology, ShanghaiTech University, Shanghai, 201210, China
2. Key Laboratory of Control of Power Transmission and Conversion (SJTU), Ministry of Education, Shanghai, 200240, China
*Corresponding author liuyu.shanghaitech@gmail.com, liuyu@shanghaitech.edu.cn

Abstract: In this paper, an improved fault location method based on magnitude measurements of voltages and sparse estimation is proposed for power networks. Compared to existing sparse estimation based fault location methods, the proposed method not only retains the advantages of sparse estimation, but also avoids the complexity of PMU installation. In this paper, the influence of fault current on the bus voltages is equivalently represented by the bus injection currents at terminals of the faulted line. With only the voltage magnitude measurements, the FISTA algorithm is adjusted to match the characteristics of the sparse estimation problem and is applied to solve for fault location. Extensive numerical experiments with different fault types, impedances and locations prove that the proposed method can accurately determine the faulted line section with a large power network, and presents high fault location accuracy within the faulted line section using only voltage magnitude measurements at a limited number of buses.

Key words: Fault location, power network, sparse estimation, voltage magnitude measurements

I. INTRODUCTION

Reliable operation of a power network is vital to ensure power supplies to customers. However, human activities, natural disasters and other emergencies often cause faults within a power network. Therefore, many fault location methods for the power network are proposed to reduce the duration of power outage and minimize the human cost in the maintenance process. The main objective of these methods is to identify the faulted branch (faulted line section) and locate the fault within the branch. They can be mainly divided into traveling wave based methods, artificial intelligence based methods and fundamental frequency phasor based methods [1].

The core idea of fault location methods based on traveling wave is to estimate the fault distance using the arrival time of wavefronts, which can be divided into single ended methods and double ended methods [2-4]. The single ended methods record the time interval between the arrival of the initial traveling wave and the reflected traveling wave to locate the fault [3]. The double ended method locates the fault point by calculating the time difference when the fault traveling wave reaches the two terminal points [4]. Synchronization among terminals are typically required. When applied to a power network, the complex reflection and refraction of traveling waves at each discontinuity of the power network will increase the complexity of the method [5,6]. Traveling wave based methods encounter great challenges when the fault inception angle is close to zero or when the fault is with high fault impedance: the wavefront intensity may not be adequate for wavefront detection. Also, traveling wave based methods usually require extremely high sampling rate (typically MHz) for accurate fault location, limiting the practicability of those methods.

Considering various applications of artificial intelligence (AI), some researches have also attempted to apply various AI based methods to fault location problems, including NN, CNN, GNN, to name a few [7,8]. Researchers also proposed physics informed AI based methods to also take the physics of the problem into account [9,10]. In general, AI based methods need to be based on a large number of high-quality fault data, which challenges the application of AI based fault location in practical scenarios.

The fault location methods based on fundamental frequency phasors build the mathematical relationship among voltage phasors, current phasors and fault location, and then solve the unknown fault location. Literature [11] completed fault location on a single transmission line based on lumped parameter model and synchronous voltage measurement. In order to further improve the fault location accuracy, the distributed parameter model was introduced in reference [12,13]. For fault location of a power network, literature [14-16] uses the known information of the power network and the lumped parameter model to apply the idea of compressed sensing to fault location. Literature [17] utilizes distributed parameter model to further improve the sparse estimation based power network fault location method. However, the above methods are based on the availability of PMUs (e.g. synchronized voltage magnitude and phase measurements), which makes the methods less applicable in practical power systems.

In fact, compared to PMU measurements, voltage magnitude measurements are more commonly installed in practical power systems. These measurements only need to calculate phasors at the local end and output phasor magnitudes, and do not require time synchronization. Therefore, this paper proposes an improved power network fault location method based on voltage magnitude measurements and sparse estimation. The method uses voltage magnitude measurements at a limited number of buses through the power network. First, the change of bus voltages due to the fault current is equivalently represented by the bus injection current at the terminal buses of the faulted line section. The fault location problem is then formulated by observing that the index of the bus injection current is sparse. Next, with the voltage magnitude measurements, the adjusted FISTA algorithm is applied to determine the faulted line section and the specific fault location. Numerical experiments prove the effectiveness and accuracy of the proposed method.

This work is sponsored by National Nature Science Foundation of China (No. 51807119) and Key Laboratory of Control of Power Transmission and Conversion (SJTU), Ministry of Education (No. 2022AB01). The support is greatly appreciated.

The remainder of this paper is arranged as follows. Section II reviews the existing sparse formulas with fully distributed parameter line model. Section III derives an improved sparse formula based on voltage amplitude, and derive the corresponding fault location method. Section IV provides numerical experiments. Section V further discusses this method. Section VI concludes this paper.

II. Review of the Existing Methods

From [16], the voltage changes of buses of the entire power network caused by the fault current at the fault location can be equivalently represented by the injection current at the terminal buses of the faulted line. For a three phase system with N buses, the voltage change vector $\Delta\mathbf{V}\in\mathbb{C}^{3N\times1}$ consists of the differences between the bus voltage phasors before and during the fault obtained by PMU for each phase of each bus. $\Delta\tilde{\mathbf{I}}\in\mathbb{C}^{3N\times1}$ is the equivalent bus injection current vector, in which the elements are nonzero at only the buses at terminals of the faulted line. With $Z_{bus,lump}\in\mathbb{C}^{3N\times3N}$, which is the impedance matrix using the lumped parameter model for transmission lines during normal operation, the formula for the current injection method is

$$\Delta\mathbf{V}=Z_{bus,\,lump}\cdot\Delta\tilde{\mathbf{I}} \tag{1}$$

Moreover, formula (1) still holds when only a limited number of PMUs are available in the system. Assume the voltage phasors of only $m(m<<N)$ buses are measured. By extracting the corresponding rows, formula (1) can be compressed as the following equation with $\left(\Delta\mathbf{V}\right)_{\mathrm{m}}\in\mathbb{C}^{3m\times1}$, $\left(Z_{bus,\,lump}\right)_m\in\mathbb{C}^{3m\times3N}$

$$\left(\Delta\mathbf{V}\right)_{\mathrm{m}}=\left(Z_{bus,\,lump}\right)_m\cdot\Delta\tilde{\mathbf{I}} \tag{2}$$

In fact, in the authors' previous publication [17], the method of fault location in a power network using sparse current injection vector is still valid when fully considering the distributed parameter line model. With $\mathrm{Z}_{bus,dis}\in\mathbb{C}^{3N\times3N}$, which is the impedance matrix of the system with full consideration of the distributed parameter model, the method above can be further improved as

$$\left(\Delta\mathbf{V}\right)_{\mathrm{m}}=\left(Z_{bus,\,dis}\right)_m\cdot\Delta\tilde{\mathbf{I}} \tag{3}$$

Due to the sparsity of the injection current vector $\Delta\tilde{\mathbf{I}}$, only a limited number of bus voltage is required to complete the fault location task by applying LASSO algorithm to the following optimization problem

$$\beta\in\underset{\beta}{\operatorname{argmin}}\frac{1}{2}\left\|\left(\Delta\mathbf{V}\right)_{\mathrm{m}}-\left(Z_{bus,\,dis}\right)_m\cdot\Delta\tilde{\mathbf{I}}\right\|_2^2+\lambda\left\|\Delta\tilde{\mathbf{I}}\right\|_1 \tag{4}$$

Assume the fault happens at the line between bus i and j as shown in Fig. 1. The rest of the system is equivalently represented by two Thevenin impedances. The faulted line section within the power network can be determined by observing the sparse nonzero elements in $\Delta\tilde{\mathbf{I}}$. The exact fault location l_{if} satisfies formula (5), where l_{ij} is the total length of the faulted line, $P=\sqrt{(R+j\omega L)\cdot j\omega C}$, and R,L,C are series resistance, series inductance and shunt capacitance per unit length, respectively.

$$\frac{\Delta\tilde{I}_i}{\Delta\tilde{I}_j}=\frac{\sinh(P\cdot(l_{ij}-l_{if}))}{\sinh(P\cdot l_{if})} \tag{5}$$

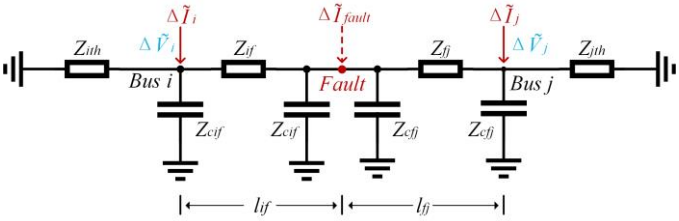

Fig. 1. Fault component network, existing method

III. Proposed Method

In section II, the existing methods based on synchronized voltage phasor measurements obtained from PMU are reviewed. For practical power systems where the PMU measurements are not available, the applications of the previous proposed methods can be limited.

In comparison, voltage magnitude measurements are more commonly installed in power networks. However, the previously proposed voltage synchrophasor based method cannot be directly used. This section will propose a method to solve the injection current with only the voltage magnitude measurements.

In each local voltage measurement, the voltage phasor can be calculated and the phase angles at the local terminal share the same time reference (without synchronization with satellite). As a result, the magnitude of $\left(\Delta\mathbf{V}\right)_m$ can be measured. Take the absolute values on both sides of the equation (3),

$$\left|\left(\Delta\mathbf{V}\right)_{\mathrm{m}}\right|=\left|\left(Z_{bus,\,dis}\right)_m\cdot\Delta\tilde{\mathbf{I}}\right| \tag{6}$$

where $\left(\mathrm{Z}_{bus,dis}\right)_m$ is a known matrix, $\left|\left(\Delta\mathbf{V}\right)_{\mathrm{m}}\right|$ is the available voltage magnitude measurement.

In this case, $\Delta\tilde{\mathbf{I}}$ can be estimated by FISTA algorithm. Define the following operators:

$re(\cdot)$: the matrix composed by extracting the real part of each element

$im(\cdot)$: the matrix composed by extracting the imaginary part of each element

$\odot$: Hadamard product

The magnitude of voltage difference can be decomposed to

$$\left|\left(\Delta\mathbf{V}\right)_{\mathrm{m}}\right|^2=re\left(\left(\Delta\mathbf{V}\right)_{\mathrm{m}}\right)^2+im\left(\left(\Delta\mathbf{V}\right)_{\mathrm{m}}\right)^2 \tag{7}$$

By defining

$$A=\left[re\left(\left(Z_{bus,\,dis}\right)_m\right)\quad-im\left(\left(Z_{bus,\,dis}\right)_m\right)\right]\in\mathbb{R}^{3m\times6N},$$

$$B=\left[im\left(\left(Z_{bus,\,dis}\right)_m\right)\quad-re\left(\left(Z_{bus,\,dis}\right)_m\right)\right]\in\mathbb{R}^{3m\times6N},$$

$$C=\left|\left(\Delta\mathbf{V}\right)_{\mathrm{m}}\right|^2\in\mathbb{R}^{3m\times1},\quad\mathbf{x}=\left[re\left(\Delta\tilde{\mathbf{I}}\right)^T\quad im\left(\Delta\tilde{\mathbf{I}}\right)^T\right]^T\in\mathbb{R}^{6N\times1},$$

formula (6) can be rewritten as

$$\left(A\cdot\mathbf{x}\right)\odot\left(A\cdot\mathbf{x}\right)+\left(B\cdot\mathbf{x}\right)\odot\left(B\cdot\mathbf{x}\right)=C \tag{8}$$

The next aim is to obtain $\Delta\tilde{\mathbf{I}}$. Due to the sparsity of $\Delta\tilde{\mathbf{I}}$, the sparsity of vector $\mathbf{x}$ can be easily proved. Hence the task turns into the following optimization problem:

$$\mathbf{x} \in \underset{\mathbf{x}}{\operatorname{argmin}} \frac{1}{2}\left\|(A\cdot\mathbf{x})\odot(A\cdot\mathbf{x})+(B\cdot\mathbf{x})\odot(B\cdot\mathbf{x})-C\right\|_2^2+\lambda\|\mathbf{x}\|_1 \quad (9)$$

where the term $\lambda\|\mathbf{x}\|_1$ is the penalty term to ensure sparsity of vector $\mathbf{x}$.

In authors' previous publication [17], the LASSO algorithm is applied to solve the optimization problem (4). However, the LASSO algorithm solves the optimization problem with relationship like $\mathbf{y}=A\mathbf{x}-b$, which is not suitable to solve (9). Therefore, in this paper, the Fast Iterative Shrinkage-Thresholding Algorithm (FISTA) is applied [18].

Let $\mathrm{f}(\mathbf{x})=(A\cdot\mathbf{x})\odot(A\cdot\mathbf{x})+(B\cdot\mathbf{x})\odot(B\cdot\mathbf{x})-C$. By defining $diag(\cdot)$ as the operator that expands the column vector to a diagonal matrix (with the column vector as the diagonal element), the analytic solution of the gradient matrix $\nabla\mathrm{f}(\mathbf{x})$ is

$$\nabla\mathrm{f}(\mathbf{x})=2\cdot diag(A\cdot\mathbf{x})\cdot A+2\cdot diag(B\cdot\mathbf{x})\cdot B \quad (10)$$

Then we can apply the FISTA algorithm to solve the optimization problem (9). To start the iterative progress, the initial step size is given as $t^1=1$, and hyperparameters L_0,λ are set as appropriate values. To calculate the value at the $(v+1)^{th}$ step from the v^{th} step, the formula is

$$\begin{aligned} t^{v+1} &= 1/2\cdot[1+\sqrt{1+4(t^v)^2}] \\ \mathbf{y}^{v+1} &= \mathbf{x}^v+(t^v-1)/t^{v+1}\left(\mathbf{x}^v-\mathbf{x}^{v-1}\right) \\ \mathbf{x}^{v+1} &= \mathrm{soft}\left[1/L_0\cdot[\nabla\mathrm{f}(\mathbf{x}^{v-1})^T\cdot\mathrm{f}(\mathbf{y}^{v+1})]+\mathbf{y}^{v+1},\lambda/L_0\right] \end{aligned} \quad (11)$$

where $\mathrm{soft}[\mathbf{x},T]=\mathrm{sign}(\mathbf{x})\odot\max(\|\mathbf{x}\|-T,0)$, and $\|\mathbf{x}\|$ takes the element-wise absolute value of $\mathbf{x}$.

After vector $\mathbf{x}$ is obtained, $\Delta\tilde{\mathbf{I}}$ can be restored by simply combining its real and imaginary part in $\mathbf{x}$. Therefore, as mentioned in Section II, the entries in $\Delta\tilde{\mathbf{I}}$ which are significantly non-zero only exist at both ends of the faulty line, while the other entries with at least an order of magnitude gap can be viewed as zero entries according to formula (12). Since the injection currents for A, B, C phases are calculated separately, the nonzero entries only occur at the faulted phase at the ends of the faulted line. Moreover, the sparsity of $\Delta\tilde{\mathbf{I}}$ should be equal to 2, 4 or 6 if only one fault occurs, and the corresponding fault types are single phase, two phase, and three phase faults, respectively. In this paper, the faulted line and phase can be selected as,

$$\left|\Delta\tilde{I}_k\middle/\max\left(\Delta\tilde{\mathbf{I}}\right)\right|\le\alpha \quad (12)$$

where α is a coefficient to differentiate the significantly non-zero entries from $\Delta\tilde{\mathbf{I}}$. Here α can be selected as $\alpha=10^3$ as an example.

To locate the fault, if the sparsity of $\Delta\tilde{\mathbf{I}}$ is 2 (corresponding to single phase faults), according to equation (5), the following optimization problem is constructed.

$$\min_{l_{if}}\mathrm{F}\left(l_{if}\right)=\left\|\frac{\Delta\tilde{I}_i}{\Delta\tilde{I}_j}-\frac{\sinh(P\cdot(l_{ij}-l_{if}))}{\sinh(P\cdot l_{if})}\right\|_2^2 \quad (13)$$

Using the Newton's Method to solve problem (13). The iterative procedure from the v^{th} step to the $(v+1)^{th}$ step is,

$$l_{if}^{v+1}=l_{if}^v-\left(H^TH\right)^{-1}H^T\left(l_{if}^v\right)\left(\frac{\sinh(P\cdot(l_{ij}-l_{if}))}{\sinh(P\cdot l_{if})}-\frac{\Delta\tilde{I}_i}{\Delta\tilde{I}_j}\right) \quad (14)$$

where $H=\dfrac{\partial}{\partial l_{if}}\left(\dfrac{\sinh(P\cdot(l_{ij}-l_{if}))}{\sinh(P\cdot l_{if})}\right)$.

Additionally, if a polyphase fault occurs, i.e. the sparsity of $\Delta\tilde{\mathbf{I}}$ is 4 or 6, the fault location can be solved for each faulted phase separately.

To summarize, the framework of the proposed method is shown in Fig. 2. Step 1 is to read the available voltage magnitude measurements to obtain $\left(\Delta\mathbf{V}\right)_{\mathrm{m}}$. Step 2 is to estimate vector $\mathbf{x}$ which contains the information of both real part and imagine part of $\Delta\tilde{\mathbf{I}}$ by FISTA algorithm, and restore $\Delta\tilde{\mathbf{I}}$. Step 3 is to observe the sparsity of $\Delta\tilde{\mathbf{I}}$ and to select the faulted line section and faulted phase. Step 4 is to use the Newton's Method to solve problem (13) and locate the fault.

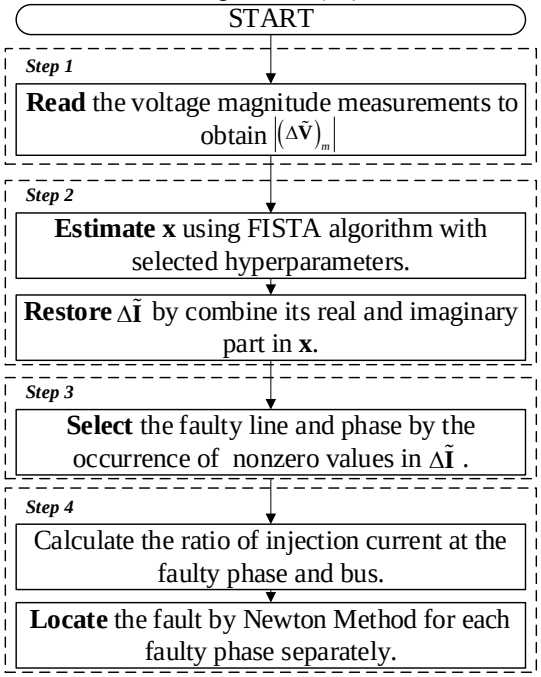

Fig. 2. Flow chart of the proposed fault location method

IV. Numerical Experiments

The IEEE118-bus standard system is established in PSCAD/EMTDC. In this system, the locations of the voltage magnitude measurements are consistent with the locations of PMUs (28 out of 118 buses) in literature [16] and [17]. The example fundamental frequency of the system is 60Hz. In this simulation, voltage phasors are extracted from the instantaneous voltage measurements according to IEEE C37.118 standard, and the voltage magnitudes are stored. To test the proposed method, the line connecting bus 30 and 38 is selected here as an example, staying the same with [17]. The total length of the line 30-38 is 265km.

A. *Faulted line section and faulted phase identification*

First, the faulted line section and the corresponding faulted phases need to be identified through the estimated bus injection current. As an example, a 0.01Ω phase A to ground occurs at 225 km from bus 30. Due to the space limitation, the injection current at bus 29 to bus 39 are shown in Fig. 3 with separated real and imaginary parts. In the figure, each bus index corresponds to three values of real or imaginary parts of $\Delta\tilde{\mathbf{I}}$, i.e., the values for phase A, B and C, respectively. The results at all other buses are all close to zero. It can be clearly observed that the sparsity of $\Delta\tilde{\mathbf{I}}$ is 2, and the significantly nonzero values only occur at phase A of bus 30 and 38. Therefore, as described in Section III, the phase A to ground fault happening at line 30-38 is correctly identified.

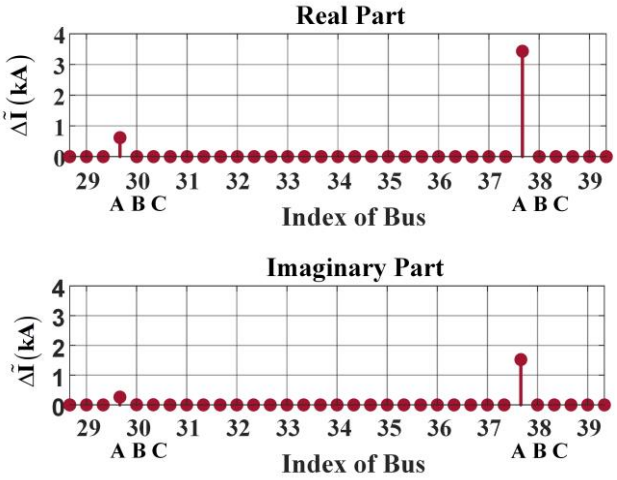

Fig. 3 Estimated real and imaginary part of the equivalent injection current, 0.01 ohm A-G fault, 225 km, line 30-38

Next, the estimated $\Delta\tilde{\mathbf{I}}$ of during a B-C fault with 0.01Ω fault resistance occurring at 225 km from bus 30 in line 30-38 is shown in Fig. 4. One can clearly observe that the sparsity of $\Delta\tilde{\mathbf{I}}$ is 4, and the significantly nonzero values occur at phase B and C of bus 30 and 38. Therefore, as described in Section III, the phase B to phase C fault happening at line 30-38 is correctly identified.

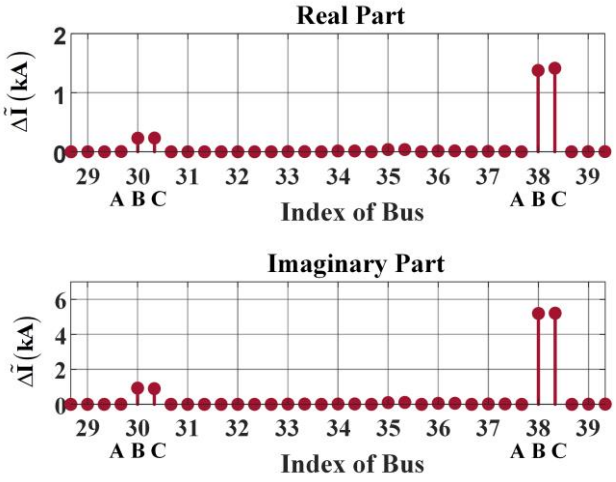

Fig. 4 Estimated real and imaginary part of the equivalent injection current, 0.01 ohm B-C fault, 225 km, line 30-38

B. *Fault location within the faulted line section*

Next, more cases are studied to verify the proposed method. Different fault types, including phase A to ground, phase B to phase C, phase B and C to ground and three phase faults are covered. Different fault resistances including 0.01Ω, 100Ω and 500Ω are applied to phase A to ground as an example for high impedance fault. The actual fault location is settled as 13km (5%), 66km (25%), 119km (45%), 172km (65%), 225km (85%) from bus 30 for each fault type. Similar as in section IV.A, the faulty line selection procedure correctly selected the faulty line for all test fault cases.

Subsequently, as described in step 4 of Fig. 2, the Newton's Method is applied to solve the optimization problem (13) with the estimated current injection phasors in step 1, 2, 3, to obtain the exact fault location. The detailed fault location results are shown as follows. The absolute fault location error is defined as

$$Absoulte\ FL\ Error = |ActualFL - EstimatedFL| \quad (15)$$

where "FL" means fault location.

The absolute fault location errors of phase A-G faults with different fault resistances (0.01Ω , 100Ω and 500Ω) are shown in Fig. 5. The averaged and maximum fault location errors are shown in the first three rows of Table I. One can observe that the maximum fault location error is lesser than 0.25 km (0.1%).

The absolute fault location errors of phase B-C faults with the fault resistance of 0.01Ω are shown in Fig. 6. The averaged and maximum fault location errors are shown in the last three rows of Table I. The maximum fault location error is lesser than 0.15 km (0.06%).

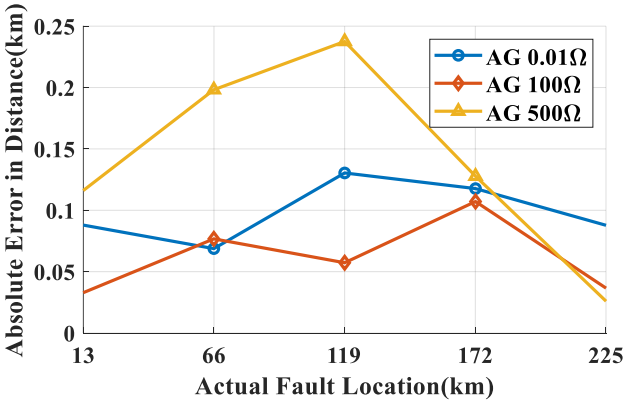

Fig. 5 Fault location results, 0.01Ω,100Ω,500Ω AG faults

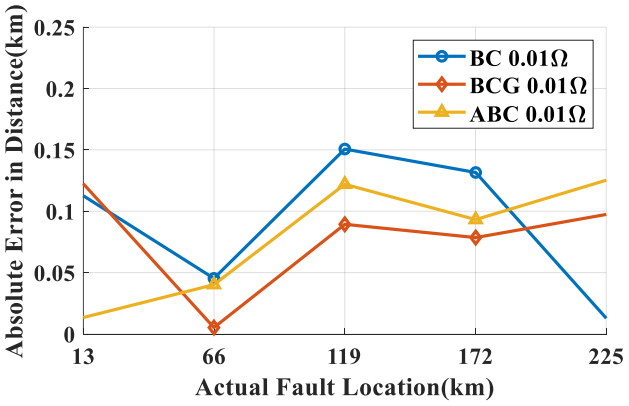

Fig. 6 Fault location results, 0.01Ω BC, BCG, ABC faults

From the above results, one can conclude that the proposed method can correctly identify the faulted line section, faulted phases, and accurately locate faults, with different fault types, fault locations, and fault resistances. Note that in this example test system, the proposed method only requires voltage magnitude measurements at 28 buses out of 118 buses for accurate fault location.

Table I

Fault type	Fault resistance	Average error(km)	Maximum error(km)
A-G	0.01Ω	0.0985	0.1304
	100Ω	0.0621	0.1071
	500Ω	0.1411	0.2375
B-C	0.01Ω	0.0906	0.1507
BC-G	0.01Ω	0.0786	0.1224
ABC	0.01Ω	0.0788	0.1253

V. Discussion

There are several important issues that need to be addressed, to ensure practicability of the proposed method.

First, the voltage magnitude measurements in this paper is $|\Delta\mathbf{V}|$; although the calculation of $|\Delta\mathbf{V}|$ does not require PMUs with satellite synchronization, it still requires local voltage phasor extraction before and during the fault, since the direct magnitude differences between the bus voltages before and during the fault is not equal to $|\Delta\mathbf{V}|$.

Second, in this paper, the FISTA algorithm is applied to solve the sparse estimation problem. However, if a random starting point is provided, it could take a relatively long time to converge to the global optimum (several hours). Moreover, the FISTA algorithm also has the risks to converge to a local optimal solution; in this case, restarting the procedure with another random point is required. Proper selection of initial values and more advanced optimization tools are valuable to ensure practicability of the proposed method.

Finally, this paper directly adopts the placement of PMUs in the existing literature for the placement of voltage magnitude measurements. Although the placement is validated via simulations, rigorous proofs of the observability of the system when using this placement of voltage magnitude measurements are still valuable to ensure that the algorithm works even in extreme scenarios. This issue will also be studied in future publications.

VI. Conclusion

This paper proposes an improved fault location method for a power network using voltage magnitude measurements at limited number of buses. First, the changes of bus voltages before and during the faults are equivalently represented by bus injection currents at the terminals of the faulted line. Afterwards, the power network model is established based on available voltage magnitude measurements. Next, with the inherent sparsity of the bus injection currents, the injection currents are estimated using the adjusted FISTA algorithm. Finally, the faulted line, faulted phases and exact fault location within the faulted line can be determined by the non-zero entries of the estimated injected current. Numerical experiments show that the proposed fault location method can correctly identify the faulted line section, faulted phases, and accurately locate faults using a limited number of bus voltage magnitude measurements throughout the power network.

References

[1] Y. Liu et al., "Dynamic State Estimation for Power System Control and Protection", *IEEE Trans. Power Syst.*, vol. 36, no. 6, pp. 5909-5921, Nov. 2021.

[2] A. O. Ibe and B. J. Cory, "A Travelling Wave-Based Fault Locator for Two- and Three-Terminal Networks", *IEEE Trans. Power Del.*, vol. 1, no. 2, pp. 283-288, April 1986.

[3] S. Shi, B. Zhu, A. Lei and X. Dong, "Fault Location for Radial Distribution Network via Topology and Reclosure-Generating Traveling Waves", *IEEE Trans. Smart Grid*, vol. 10, no. 6, pp. 6404-6413, Nov. 2019.

[4] S. Azizi, M. Sanaye-Pasand, M. Abedini and A. Hasani, "A Traveling-Wave-Based Methodology for Wide-Area Fault Location in Multiterminal DC Systems", *IEEE Trans. Power Del.*, vol. 29, no. 6, pp. 2552-2560, Dec. 2014.

[5] C. Y. Evrenosoglu and A. Abur, "Travelling wave based fault location for teed circuitsx", *IEEE Trans. Power Del.*, vol. 20, no. 2, pp. 1115-1121, April 2005.

[6] Yun'an Xu, Yu Liu*, Yiqi Xing, Yuan Nie and Wentao Huang, "Power Network Fault Location Using Traveling Waves and Continuous Wavelet Transform", *IEEE Power & Energy Society General Meeting (PESGM)*, 2022.

[7] W. Li, D. Deka, M. Chertkov and M. Wang, "Real-Time Faulted Line Localization and PMU Placement in Power Systems Through Convolutional Neural Networks", *IEEE Trans. Power Syst.*, vol. 34, no. 6, pp. 4640-4651, Nov. 2019.

[8] K. Chen, J. Hu, Y. Zhang, Z. Yu and J. He, "Fault Location in Power Distribution Systems via Deep Graph Convolutional Networks", *IEEE J. Sel. Areas Commun.*, vol. 38, no. 1, pp. 119-131, Jan. 2020.

[9] Yiqi Xing, Yu Liu*, Binglin Wang, Lihui Yi, and Xuming He, "Physics-Informed Data-Driven Transmission Line Fault Location Based on Dynamic State Estimation", *IEEE Power & Energy Society General Meeting (PESGM)*, 2022.

[10] Yiqi Xing, Yu Liu*, Yuan Nie, Rongjie Li and Xuming He, "Data-Driven Transmission Line Fault Location with Single-Ended Measurements and Knowledge-Aware Graph Neural Network", *IEEE Power & Energy Society General Meeting (PESGM)*, 2022.

[11] S. M. Brahma and A. A. Girgis, "Fault location on a transmission line using synchronized Voltage measurements", *IEEE Trans. Power Del.*, vol. 19, no. 4, pp. 1619-1622, Oct. 2004.

[12] Joe-Air Jiang, Jun-Zhe Yang, Ying-Hong Lin, Chih-Wen Liu and Jih-Chen Ma, "An adaptive PMU based fault detection/location technique for transmission lines. I. Theory and algorithms", *IEEE Trans. Power Del.*, vol. 15, no. 2, pp. 486-493, April 2000.

[13] Y Liu, et. al, "Fault Location Algorithm for Non-Homogeneous Transmission Lines Considering Line Asymmetry", *IEEE Trans. Power Del.*, vol. 35, no. 5, pp. 2425-2437, Oct. 2020.

[14] M. Majidi, A. Arabali and M. Etezadi-Amoli, "Fault Location in Distribution Networks by Compressive Sensing", *IEEE Trans. Power Del.*, vol. 30, no. 4, pp. 1761-1769, Aug. 2015.

[15] Q. Jiang, X. Li, B. Wang and H. Wang, "PMU-Based Fault Location Using Voltage Measurements in Large Transmission Networks", *IEEE Trans. Power Del.*, vol. 27, no. 3, pp. 1644-1652, July 2012.

[16] G. Feng and A. Abur, "Fault Location Using Wide-Area Measurements and Sparse Estimation", *IEEE Trans. Power Syst.*, vol. 31, no. 4, pp. 2938-2945, July 2016.

[17] Yixiong Jia, Yu Liu*, Binglin Wang, Dayou Lu and Yuzhang Lin, "Power Network Fault Location with Exact Distributed Parameter Line Model and Sparse Estimation", *Electric Power System Research (EPSR)*, early access, 2022.

[18] A. Beck and M. Teboulle, "A fast Iterative Shrinkage-Thresholding Algorithm with application to wavelet-based image deblurring", *Proc. IEEE ICASSP*, pp. 693-696, April 2009.